Computational Materials Science 50 (2010) 356–362

Contents lists available at ScienceDirect

Computational Materials Science

journal homepage: www.elsevier.com/locate/commatsci

# Surface stability of potassium nitrate ($KNO_3$) from density functional theory

O.M. Løvvik [a,b,*], T.L. Jensen [c,**], J.F. Moxnes [c], O. Swang [a,d], E. Unneberg [c]

[a] SINTEF Materials and Chemistry, PO Box 124, Blindern, NO-0314 Oslo, Norway
[b] Department of Physics, University of Oslo, PO Box 1048, Blindern, N-0316 Oslo, Norway
[c] Norwegian Defence Research Establishment, PO Box 25, NO-2027 Kjeller, Norway
[d] Department of Chemistry, University of Oslo, PO Box 1033, Blindern, N-0315 Oslo, Norway

ARTICLE INFO

*Article history:*
Received 7 April 2010
Received in revised form 25 August 2010
Accepted 26 August 2010

*Keywords:*
Potassium nitrate
Surface energy
Density functional theory

ABSTRACT

Potassium nitrate has been studied by accurate DFT calculations. The bulk crystal structure and electronic structure were calculated and compared to previous studies. In addition, the surface stability of various faces was quantified, confirming that the {0 0 1} face has the lowest surface energy of 0.19 $Jm^{-2}$. Other surfaces terminated by nitrate ions exhibited reconstructions upon relaxation, rotating the ions into an orientation parallel to the surface plane.



## 1. Introduction

Potassium nitrate ($KNO_3$) has many applications, e.g. as a fertilizer, as an oxidizing agent in pyrotechnics, and in food preservation. The metastable γ phase has been extensively studied due to its ferroelectric properties [1–5]. It has, however, been difficult to take any practical advantage of this, due to the lack of stability [6–9].

$KNO_3$ crystallizes at room temperature into the α phase (also called phase II). For a long time it was believed that this phase belonged to the space group *Pmcn* (orthorhombic, with $Z = 4$) [10–12]. However, a neutron diffraction study by Adiwidjaja and Pohl demonstrated that the crystal structure actually consists of a $2 \times 2 \times 1$ supercell of the *Pmcn* unit cell, with $Z = 16$ and within the space group $Cmc2_1$ [13]. The crystal structure transforms into the β phase (I) at around 128 °C when heated, and passes through the ferroelectric γ phase (III) between 124 and 110 °C upon cooling. A number of phases also exists at lower temperatures [14,15]. Transitions between these phases have been extensively studied by a variety of techniques [7,16–41].

The growth of $KNO_3$ crystals has been examined by several authors [42–46], and it has been shown that the {0 0 1} face has the lowest surface energy [43]. Other crystal faces have also been observed, including the {0 1 0}, {1 0 0}, {1 1 0}, {0 1 1}, {0 2 1}, {0 1 2}, and {1 1 1} faces. An overview of the possibilities of different kinds of growth is given by Rolfs et al. [43].

Previous theoretical studies on this system have focused on the ferroelectric properties of the γ phase [5,47,48] and on phase transitions [30,49]. The Hartree–Fock study by Aydinol et al. also presented calculations of bonding characteristics and the structural stability of various phases of $KNO_3$ [5]. The present contribution has a slightly different focus. We report a detailed computational study of the bulk electronic structure of the α phase of $KNO_3$, followed by an investigation of the stability of various surfaces. All calculations are performed within the scope of density functional theory (DFT) using a plane wave description of the electron density and periodic boundary conditions.

## 2. Methodology

Calculations were performed within density functional theory (DFT) as implemented in the Vienna *ab initio* simulation package (VASP) [50,51], using the PBE generalized gradient approximation (GGA) density functional [52]. The projector augmented wave (PAW) method [53] was used to represent the electron density. This is a generalization of the linearized augmented plane wave (LAPW) and the pseudopotential (PP) methods, with reliability comparable to that of LAPW and efficiency close to that of PP methods [53]. All calculations were spin unrestricted, allowing for spin polarization. Despite this, no net spin density was seen for any of the systems described herein.

DFT calculations were also performed applying the *ab initio* simulation package Quantum Espresso (QE) v4.0.3 [67], using the BLYP

* Corresponding author at: SINTEF Materials and Chemistry, PO Box 124, Blindern, NO-0314 Oslo, Norway.
** Corresponding author.
*E-mail addresses:* ole.martin.lovvik@sintef.no (O.M. Løvvik), tomas-lunde.jensen@ffi.no (T.L. Jensen).

0927-0256/$ - see front matter © 2010 Elsevier B.V. All rights reserved.
doi:10.1016/j.commatsci.2010.08.027

functional and norm-conserving pseudopotentials. The QE calculations allowed no spin polarization.

The density of k points in the reciprocal space integration was always kept below 0.2 per $Å^{-1}$. As an example, a gamma-centred $4 \times 2 \times 4$ mesh was used for the *Pmcn* bulk unit cell. Convergence tests up to an $8 \times 6 \times 8$ mesh confirmed that the uncertainty in total energy resulting from the chosen sampling was below 1 meV per unit cell. For slab calculations, only the gamma point was used in the vacuum direction. The tetrahedron method with Blöchl corrections was used to smear partial occupancies near the Fermi level. The criterion for self-consistence was a change in total electronic energy of less than $10^{-6}$ eV between consecutive electron density iterations. The QE calculations used the same density of k points.

Computer codes for plane-wave calculations have often built in default values for energy cut-off. For $KNO_3$, the default value would be 400 eV for the standard (soft) potentials in VASP. However, we expected an unusually strong perturbation of the N and/or O atoms upon formation of nitrate groups, and therefore conducted convergence tests of the total energy as a function of the kinetic energy cut-off $E_c$. Indeed, as seen in Fig. 1(a), the total energy changes dramatically with increasing $E_c$. The total energy is not properly converged (defined here as changing by less than 1 meV when increasing $E_c$ by 50 eV) until $E_c = 1250$ eV. Even at this point the total energy continues to drop, and is 2.5 meV lower when $E_c = 1500$ eV. This indicates the existence of electron density changes uncommonly close to the atomic nuclei, and we found it necessary to repeat the test with harder potentials (smaller frozen core and higher plane wave cut-offs). These results are also shown in Fig. 1(a), and again we see that the default $E_c$ (which is much higher (750 eV) for the hard potentials) is clearly insufficient to achieve convergence. This time, however, proper convergence is obtained at 950 eV, and the change in total energy is less than 0.1 meV when increasing $E_c$ further to 1100 eV. We investigated the same convergence behaviour for QE, this is shown in Fig. 1(b). The total energy convergence with respect to $E_c$ is even worse for the norm-conserving potentials. We have plotted the behaviour for two different choices of the cut-off energy for charge $E_{charge}$; $E_{charge} = 4\ E_c$ (default) and $E_{charge} = 2\ E_c$. Proper convergence has not been found in any of the cases, even when $E_c$ is increased to more than 2000 eV (note the different scales on the axes of Fig. 1 (a) and (c)).

This means that the convergence criterion we proposed (1 meV change of total energy/50 eV increase of $E_c$) may be too strict. After all, we are usually interested in relative energies, not the absolute total energy. To test another option, we plotted the calculated pressure of the experimental cell (which is non-zero because the applied density functional fails to predict the exact magnitude of the lattice parameters) as a function of $E_c$. The calculated pressure is an important quantity when performing automatic relaxation of the unit cell size (and shape), which can be used to search for unknown crystal structures [54]. For VASP, the pressure is apparently already converged (changes less than 1 kbar when $E_c$ is increased by 50 eV) at 500 eV for the soft potentials (Fig. 1(b)). When using hard potentials, similar convergence is reached at a cut-off of 950 eV. In the case of QE using norm-conserving pseudopotentials, we see that a cut-off of 1360 eV is necessary to obtain proper convergence of the pressure (Fig. 1(d)). In this case we can clearly see that using $E_{charge} = 2\ E_c$ is necessary to obtain convergence; when the default value of $E_{charge} = 4\ E_c$ is used, the pressure seems to diverge when $E_c$ is increased further.

Another important set of parameters is the calculated forces, which are used when optimizing the ionic positions. We checked numeric convergence of the forces with respect to $E_c$ in a similar vein as above. The convergence criterion was now that the force changes should be less than 0.05 eV/Å when $E_c$ is increased with 50 eV. In the case of VASP we found converged of the forces for $E_c = 450$ and 600 eV for the soft and hard potentials, respectively. QE exhibited converged forces at $E_c = 1224$ eV when $E_{charge} = 2\ E_c$; when $E_{charge} = 4\ E_c$ the forces were converged at 1496 eV.

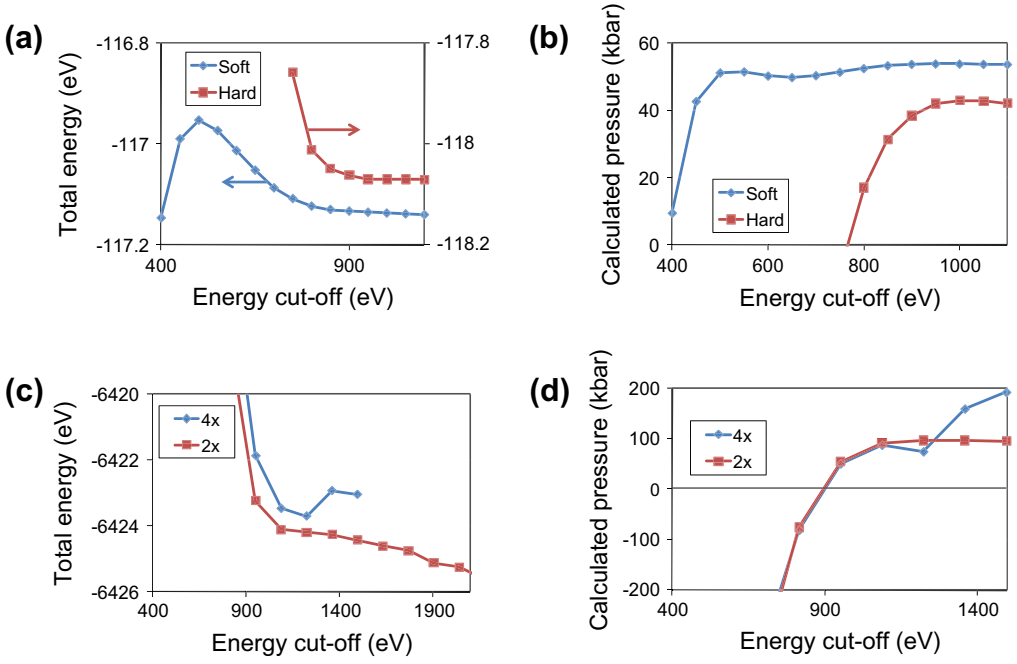


**Fig. 1.** Convergence of the calculated electronic total energy (a and c) and the calculated pressure (b and d) as a function of the energy cut-off of the kinetic energy plane wave expansion. The upper panels present VASP calculations with blue diamonds denoting standard (soft) potentials, and red squares denoting potentials with smaller frozen core and higher cut-offs (hard). The lower panels present data from QE calculations, with two different values of the charge density energy cut-off (augmentation cut-off); 4 and 2 times that of the kinetic energy cut-off, represented by blue diamonds and red squares, respectively. Lines are drawn as guides to the eye only. (For interpretation of the references to colour in this figure legend, the reader is referred to the web version of this article.)